Journal of Quantitative Spectroscopy & Radiative Transfer 202 (2017) 90–97

Contents lists available at ScienceDirect

Journal of Quantitative Spectroscopy & Radiative Transfer

journal homepage: www.elsevier.com/locate/jqsrt

Absorption enhancement of aged black carbon aerosols affected by their microphysics: A numerical investigation

Xiaolin Zhang[a,b,c], Mao Mao[a,b,c,*], Yan Yin[a,b], Bin Wang[a,c]

[a] Earth System Modeling Center, Collaborative Innovation Center on Forecast and Evaluation of Meteorological Disasters, Key Laboratory for Aerosol-Cloud-Precipitation of China Meteorological Administration, Joint International Research Laboratory of Climate and Environment Change, Nanjing University of Information Science & Technology, Nanjing, 210044, China
[b] School of Atmospheric Physics, Nanjing University of Information Science & Technology, Nanjing, 210044, China
[c] International Pacific Research Center, University of Hawaii at Manoa, Honolulu, HI, 96822, USA

ARTICLE INFO

Article history:
Received 27 March 2017
Revised 9 June 2017
Accepted 21 July 2017
Available online 24 July 2017

Keywords:
Aged aerosol
Absorption enhancement
Lensing effect
Numerical investigation

ABSTRACT

An idealized spherical model with black carbon (BC) aggregates fully coated by sulfate is developed to study the absorption enhancement (E_{ab}) of polydisperse BC aerosols, which is numerically calculated by the multiple-sphere T-matrix method (MSTM). The aim of this study is to evaluate the effects of aerosol microphysics on the absorption enhancement of fully coated BC particles. The E_{ab} values of accumulation concentric coated BC aggregates with different BC fractal dimensions vary within 2%, while those of coarse coated BC aggregates can alter up to 20% depending on shell-core ratio D_p/D_c (spherical equivalent particle diameter divided by BC core diameter). The BC position inside coating can result in an E_{ab} decrease of fully coated BC aggregates up to approximately 15% and 20% in the accumulation and coarse modes, respectively. Compared with the concentric spherical structure, the off-center coated BC aggregates shows similar E_{ab} with a difference less than 9% in the accumulation mode, whereas it can lead to up to 31% reductions in E_{ab} in the coarse mode. The absorption enhancement of aged BC is sensitive to particle size distribution, and it decreases as particles becomes larger in accumulation mode, whereas the reverse is true in coarse mode. For BC aggregates fully coated with a very thin layer sulfate at different size distributions, E_{ab} values are generally in ranges of 1.5–1.8 and 1.3–1.4 in accumulation and coarse modes, respectively, while with coating reaching $D_p/D_c = 2.7$, their values range from 1.7–2.4 and 2.0–2.1 in accumulation and coarse modes, respectively. Our study indicates that, larger D_p/D_c with BC aggregates not close to the coating boundary, or BC position closer to particle geometric center enhance BC lensing effect, whereas BC aggregates near the boundary of heavy coating may not further enhance lensing effect significantly with increased coating fraction.

1. Introduction

Black carbon (BC) aerosols are largely generated due to fossil fuel demands, unless clean renewable energy sources [1,2] are widely utilized. Black carbon has been identified as the second most important anthropogenic global warming agent in the atmosphere by virtue of their strong absorption of solar radiation and their role in cloud formation [3,4]. The BC climate effects are significantly dependent on the mixing state (i.e., externally or internally mixing with other aerosol species) [5,6], and atmospheric aging by coating with secondary components induces BC absorption enhancement (E_{ab}) [7,8]. In light of the complex morphology and mixing structure, our understanding of BC properties, including the absorption enhancement of aged BC, is still limited, making BC one of the biggest uncertainties in the estimation of aerosol radiative forcing [9,10].

Freshly emitted BC aerosols are mostly hydrophobic and externally mixed with other particulates [11], and soon after, BC agglomerates to form aged BC aggregates due to multi-phase processes in the atmosphere [12]. The observations show that, during the aging process, BC becomes coated with other components, including heterogeneous reactions with gaseous oxidants [13], coagulation with preexisting particulates [14], and condensation of sulfate, organics and nitrate [15]. Meanwhile, BC aggregates may undergo considerable geometry restructuring and become compact after coated [11]. The coatings on BC can enhance the absorption above that of uncoated BC particles through the so-called 'lensing effect', which has been confirmed by theoretical calculations using Mie theory [5,16,17] and laboratory measurements under controlled conditions [18–21]. The enhancement of absorption can result in significant bias in ambient BC measurements [22,23],

* Corresponding author.
E-mail addresses: xlnzhang@nuist.edu.cn (X. Zhang), mmao@nuist.edu.cn (M. Mao).

http://dx.doi.org/10.1016/j.jqsrt.2017.07.025
0022-4073/

and further, lead to uncertainties in assessing the radiative effect [24,25].

Many field measurements have been carried out to reveal the variation of BC absorption during atmospheric aging processes. Knox et al. [26] observed an absorption enhancement up to 45% because of BC coating in downtown Toronto, Canada. Naoe et al. [27] presented that the coating enhance BC absorption by a factor of 1.1–1.4 with a larger enhancement for thicker coating at a suburban site in Japan. The absorption enhancements rising from 1.4 ± 0.3 in fresh combustion emissions to ~3 for aged BC aerosols are found in a regional rural site over the North China Plain (NCP) [28]. However, Cappa et al. [29] reported a negligible absorption enhancement of only 6% for ambient BC particles under a variable mixing state based on direct measurements over California, USA. This implies that the absorption enhancement of BC due to coating is rather complicated in ambient air, which may be dependent on particle size distribution, composition ratio, and coating morphology affected by emission sources and aging processes.

Numerical modeling is a powerful method to improve our understanding of the complex absorption enhancement of aged BC aerosols. Core-shell Mie theory calculations employed by many current climate models, assume coated BC particles with a concentric spherical configuration and indicate absorption enhancements up to 3 being plausible [16,17]. Thus, the state-of-the-art climate models typically either compute an absorption enhancement on the basis of simplified mixing-state assumptions or assume a constant value of ~1.5 for BC absorption calculations [30–33]. Nevertheless, the simple concentric spherical core-shell model cannot adequately represent realistic BC-containing particles in the atmosphere. He et al. [34] calculated the absorption enhancement of BC coated by sulfuric acid at three monodisperse sizes (i.e., mobility diameters of 155, 245 and 320 nm) with different morphologies to capture BC aging in laboratory experiments. Some other coated BC models representing more realistic morphologies are built to study their optical properties [e.g., 35, 36], while corresponding calculations relevant to absorption enhancement due to BC coating show generally qualitative results.

Recently, more and more observations related to the composition ratio and mixing structure of aged BC aerosols are presented. Based on the SP2 (single-particle soot photometer) measurements of BC spherical equivalent core diameter (D_c) and coating thickness, observed values of D_p/D_c (particle diameter divided by BC core diameter) are 1.1–2.1 in London [37] and 2.1–2.7 in Beijing [38]. Among aged BC coating materials, sulfates are found to be primary drivers of enhanced BC absorption in China [28], and the large sulfate formation rate is induced by the aqueous oxidation of SO_2 by NO_2 under polluted environments [39]. About 48.6% BC particles are observed to be coated with non-refractory materials during polluted period in northwestern China [40]. The observations from China et al. [41] quantify that ~50% BC aerosols emitted from biomass burning are heavily coated (embedded), ~34% are partly coated, ~12% have inclusions and ~4% are bare. Similar results with fully and partly coated morphologies dominated are observed for aged BC particles at a remote marine free troposphere site in Portugal, where often receives long-range transported air masses from North America, Africa or Europe [42]. Some studies show that BC aerosols externally attached to or partially encapsulated in weakly absorbing materials have E_{ab} of ~1, i.e., absorption showing no obvious increase relative to uncoated BC particles [34,43,44]. This is probably due to that externally attached and partially coated BC geometries lack of efficient lensing effect, and that weakly absorbing coating materials block the photons from behind BC, producing a shadowing effect [45]. Thus, BC particles fully coated with weakly absorbing materials account for the absorption enhancement significantly, which is still under discussion. With more recent observations shown, a more reliable and quantitative simulation of the absorption enhancement of aged BC aerosols becomes urgent, which will benefit our understanding of the mechanism responsible for the model-observation discrepancies.

Here, we build a simple model to systematically account for the impacts of aerosol microphysics of aged BC particles on their absorption enhancement based on our current understanding. The model representing aged BC particles, and the numerical method used to calculate their absorption properties and absorption enhancements are introduced in Section 2. Section 3 presents the effects of aerosol microphysics, including composition ratio, coating morphology and size distribution, on the absorption enhancement of coated BC particles. The sensitivity evaluations of aged BC absorption enhancement due to uncertainties of BC refractive index are also discussed in Section 3, and Section 4 concludes the work.

2. Methodology

2.1. Aged BC model

The observations indicate that freshly emitted BC particles usually exist as loose cluster-like aggregates, having numerous similar-sized spherical monomers [e.g., 46]. The fractal aggregates have been successfully utilized to construct these freshly BC aggregation geometry, obeying the well-known statistical scaling law [e.g., 47]:

$$N = k_f \left(\frac{R_g}{a} \right)^{D_f}, \tag{1}$$

where N is the monomer number of an aggregate, a is the monomer radius, and k_f and D_f are the fractal prefactor and fractal dimension, respectively, controlling the aggregate structure. The aggregate becomes more compact, as k_f or D_f increases. R_g is the gyration radius, measuring the overall spatial size of an aggregate, and is defined as

$$R_g = \sqrt{\frac{1}{N} \sum_{i=1}^{N} r_i^2}, \tag{2}$$

where r_i denotes the distance of the ith monomer from the whole aggregate mass center.

The observations also show that these freshly emitted BC aggregates tend to be coated with secondary aerosol compounds through coagulation and condensation with the time going [e.g., 48,49]. During this aging process, most BC particles are thickly coated, and their chain-like aggregates tend to collapse into more compact clusters [21,50]. The fractal dimensions for fresh BC aggregates are generally less than 2, while they are close to 3 for aged BC aerosols [51]. There is sufficient evidence that aged BC aerosols can be overall particle spherical, and some microscopic images do show this geometry [e.g., 21,52,53]. Meanwhile, the simple spherical coatings on BC have similar effects on optical properties to those based on more complicated coating structure [35,36]. BC coating components mainly consist of sulfate, nitrate, ammonium and organics [54], and we select sulfate as the weakly absorbing coating material, since it is the primary driver of enhanced BC absorption over China [28,39]. Therefore, the simple sphere with BC fractal aggregate coated with sulfate, is considered to build a realistic aged BC particle model for efficient optical simulation here. This study considers the aged BC particles with sulfate fully coated, which is illustrated in Fig. 1.

To construct this homogeneous internal-mixed particle, we first generate a BC fractal aggregate and then add a spherical sulfate coating. For the BC aggregates, the value of k_f is set to be 1.2 based on Sorensen [47]. The radius a of BC aggregate monomers varies over a range of about 10–25 nm [55], while the monomer number N is observed to vary up to approximately 800 [56]. Since

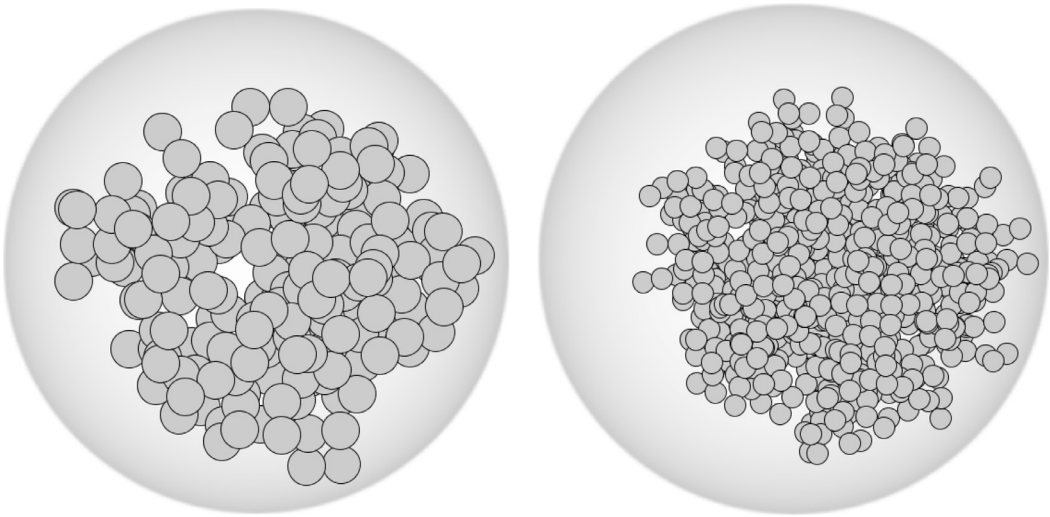

Fig. 1. Examples of modeled aged black carbon geometries. The fractal black carbon aggregates, containing 200 (left) and 800 (right) monomers, coated with sulfate are applied to model accumulation and coarse particles, respectively.

the monomer size has a rather weak effect on BC scattering and absorption after D_f being fixed [34,45], we choose two N values of 200 and 800 as examples for accumulation and coarse particles, respectively, and compare three D_f values of 2.6, 2.8 and 2.98 for aged BC aggregates. A tunable particle-cluster aggregation algorithm from Skorupski et al. [57] is used to generate BC aggregates with given fractal parameters.

2.2. Numerical simulation of bulk absorption properties and E_{ab}

The multiple-sphere T-matrix method (MSTM) [58], one of the most efficient and accurate models, is used to numerically calculate the random-orientation absorption properties of aged BC aggregates in this study. The MSTM considering a cluster of spheres, is in the framework of the T-matrix method, with the only limitation that the spherical surfaces are nonoverlapping [59]. It employs the addition theorem of vector spherical wave functions to account for mutual interactions among the multiple-sphere system, and its T-matrix for deriving particle absorption properties can be achieved from the individual spheres [58]. The absorption properties of randomly oriented aerosols can be obtained from the MSTM without numerical averaging over particle orientations, which is different from most other numerically exact models. The robust and popular MSTM code has already been widely utilized for numerous numerical investigations of the absorption properties of fractal aggregates [e.g., 60,61].

For atmospheric applications, the bulk optical properties averaged over a certain particle size distribution are meaningful, and an ensemble of BC aggregates with different sizes but the same sulfate coating fraction is considered in this study. The internal-mixed BC-sulfate particles are assumed to follow a lognormal size distribution in the form of:

$$\mathrm{n}(r) = \frac{1}{\sqrt{2\pi}\, r \ln(\sigma_g)} \exp\left[-\left(\frac{\ln(r) - \ln(r_g)}{\sqrt{2}\ln(\sigma_g)} \right)^2 \right], \tag{3}$$

where r_g is the geometric mean radius, and σ_g is the geometric standard deviation [e.g., 49,62]. As particles in accumulation and coarse modes contribute most of the light absorption, we only consider the coated BC in both modes. To better understand the absorption enhancement of aged BC at different particle size mode, we use the size distributions in accumulation and coarse modes separately, which are similar to those applied in the aerosol-climate models [63]. In this study, the r_g value is considered to be 0.075 μm [64], whilst σ_g values of 1.59 and 2.0 are assumed for accumulation and coarse BC-sulfate internal mixtures, respectively [63]. With the particle size distribution given, the bulk absorption cross section can be easily obtained by following equation:

$$\langle C_{abs} \rangle = \int_{r_{\min}}^{r_{\max}} C_{abs}(r) n(r) d(r) \tag{4}$$

In accumulation mode, the minimum and maximum radii are set to be $r_{\min} = 0.05\,\mu$m and $r_{\max} = 0.5\,\mu$m, respectively. In coarse mode, $r_{\min}$ is 0.5 μm while $r_{\max}$ is set to be 2.5 μm, since ambient aerosols with diameter larger than 5 μm is few [65–69] and individual aerosol samples for measuring mixing structures also show particle size less than 5 μm [46]. With the ensemble-averaged absorption cross section obtained, the absorption enhancement E_{ab} is given following the equation below:

$$E_{ab} = \frac{C_{particle}}{C_{bare\ BC}}, \tag{5}$$

where $C_{particle}$ is the bulk absorption cross section of the BC aggregates coated with sulfate, while $C_{bare\ BC}$ is the bulk absorption cross section of the same BC aggregates but without sulfate coating (bare BC).

This study considers an incident wavelength of 550 nm, and corresponding BC and sulfate refractive index are $1.85 - 0.71i$ [55] and $1.52 - 5.0 \times 10^{-4} i$ [70], respectively. Based on the D_p/D_c measurements of coated BC in London and Beijing [37,38], this study chooses D_p/D_c ranges of 1.1–2.7 for aged BC aggregates. It should be noted that, some small D_p/D_c values might not be used, as we only study the cases for BC aggregates with sulfate completely coated (i.e., BC aggregates fully inside sulfate). Based on the inhomogeneous aged BC model defined, which shows quite realistic geometries and great flexibility, and the efficient MSTM, it is possible to study the absorption enhancement of aged BC aerosols affected by their microphysics, including coating morphologies, composition ratios, BC refractive index and size distributions, with more details.

3. Results and discussion

3.1. Effect of aged BC morphologies on E_{ab}

The study focuses on the influence of the microphysics of aged BC on its absorption enhancements, and, therefore, the properties

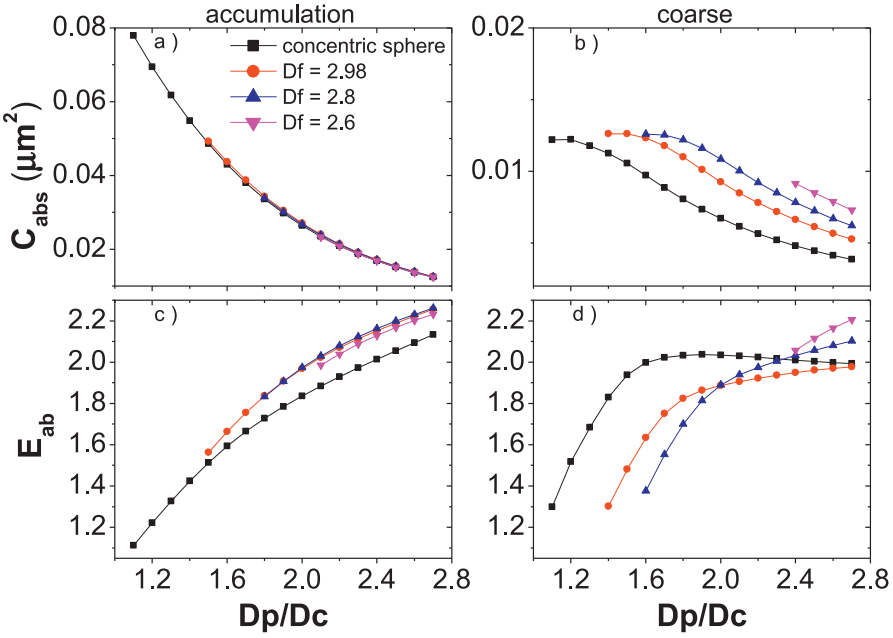

Fig. 2. Absorption cross section (C_{abs}) and absorption enhancement (E_{ab}) of BC aggregates with sulfate coated as functions of shell/core ratio (D_p/D_c, sulfate-BC particle diameter/spherical volume-equivalent BC core diameter), for accumulation (left two) and coarse (right two) modes, respectively. Four BC morphologies with BC mass center located at BC-sulfate particle geometric center are considered, including concentric core-shell (black squares), and aggregates with fractal dimensions of 2.98 (red circles), 2.8 (blue up-triangles) and 2.6 (magenta down-triangles). (For interpretation of the references to color in this figure legend, the reader is referred to the web version of this article.)

of the microphysics are our interest. The aged BC light absorption and its absorption enhancement depend not only on particle composition ratio (i.e., BC content, or D_p/D_c) but also on particle morphology (i.e., the physical arrangement of BC with respect to other components within a given particle). With sulfate coating geometry fixed and BC fully coated, we will consider two other morphological factors: BC geometry and BC position inside sulfate coating.

To show the effect of BC geometry on aged BC absorption, the concentric core-shell structures (i.e., mass centers locating at coating center) with inside BC aggregates having fractal dimensions of 2.6, 2.8 and 2.98, as well as a spherical BC core, are considered. Fig. 2 compares the bulk absorption properties of aged BC aerosols with different BC geometries at different composition ratios. The properties are averaged over an ensemble of BC-sulfate internal-mixed particles with aforementioned size distributions for accumulation and coarse modes separately. Theoretical results with a popular BC refractive index of $1.85-0.71i$ and a fractal prefactor of 1.2 described before are used for study unless stated otherwise. It is expected that, as the BC content increases (i.e., D_p/D_c decreases), C_{abs} becomes much stronger. With D_p/D_c varying from 2.7 to 1.1, the absorption cross sections become almost 8 times larger from $\sim 0.01\,\mu m^2$ to $\sim 0.08\,\mu m^2$ in accumulation mode, whilst their values increase only about 3 times in coarse mode (see Fig. 2a and b). With mass-center positions of different BC geometries fixed within spherical sulfate coating, the overall particle C_{abs} values are not sensitive to their inside BC geometries for accumulation aerosols. Whereas, in coarse mode, coated BC particles with small BC aggregate fractal dimension have larger C_{abs}, followed by particles with large BC fractal dimension, and concentric spherical aged BC particles show the lowest absorption at the same BC content. The concentric spherical core-shell structure decreases C_{abs} of coarse aged BC by 10–50% depending on BC content and fractal dimension, compared with the concentric aggregate core-shell structure (i.e., concentric core-shell structure with an aggregate BC core). This is in line with the conclusion presented in Kahnert et al. [71] that differences in BC absorption between concentric spherical core-shell and encapsulated aggregate structures strongly depends on particle size, BC volume fraction and wavelength.

As depicted in Fig. 2c and d, the absorption enhancement of BC aggregates coated with sulfate is sensitive to both composition ratio and BC geometry. For a BC fractal dimension of 2.98, with D_p/D_c increases from possible minimum values (very thin coating) to 2.7 (heavy coating), E_{ab} variations of 1.6–2.3 and 1.3–2.0 are obtained in accumulation and coarse modes, respectively. The E_{ab} increases with D_p/D_c increasing at three different fractal dimensions, indicating small BC content or large sulfate coating fraction enhance lensing effect. It should be noticed that, the E_{ab} for coarse concentric spherical aged BC decreases with D_p/D_c increasing when D_p/D_c is larger than 2.0. The influence of BC geometry on coated BC absorption enhancement of is relatively complex. For aggregate BC geometry in concentric core-shell structure, E_{ab} of coated BC in accumulation mode is less sensitive to its BC fractal dimension compared to coarse mode. The E_{ab} values of accumulation aged BC aerosols with different BC fractal dimensions vary within 2%, while those of coarse coated BC aggregates can alter up to 20%. In coarse mode, large BC aggregate fractal dimension tends to decrease E_{ab} for coated BC containing small BC content (e.g., D_p/D_c larger than 2.4), whereas the reverse is true for aged BC with large BC fraction (e.g., D_p/D_c less than 2.0). For concentric spherical core-shell structure, E_{ab} values of accumulation aged BC are smaller than those of corresponding concentric aggregate core-shell structure by 3–7%, depending on D_p/D_c and BC fractal dimension. In contrast, coarse aged BC particles with a concentric spherical structure can produce significant larger E_{ab} than coated BC aggregates by up to 45%, when D_p/D_c is less than 2.2. Compared to concentric aggregate core-shell structure, the accumulation aged BC with a concentric spherical structure produces similar C_{abs} but lower E_{ab}, indicating, in accumulation mode, spherical BC core geometry underestimating lensing effect and bare BC aggregates having smaller absorption than volume-equivalent sphere.

The simulations discussed above assume aged BC with a concentric core-shell structure, which does not always stand for realistic particles, while coated BC with an off-center core-shell struc-

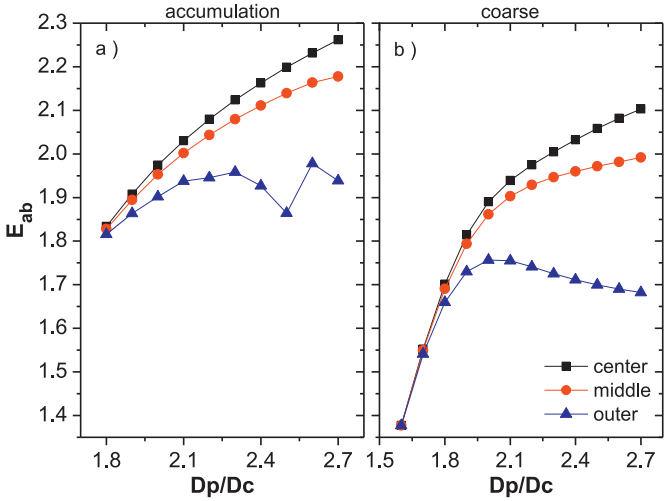

Fig. 3. Absorption enhancement (E_{ab}) of aged BC aggregates (BC fractal dimension of 2.8) with different coating positions as a function of shell/core ratio (D_p/D_c), for accumulation (left panel) and coarse (right panel) modes, respectively. Three BC coating morphologies are considered, i.e., a core-shell with BC mass center located at particle geometric center (black squares), and two off-center core-shell structures including BC aggregates lying at middle position of a particle radius (red circles) and outer position close to spherical boundary (blue triangles). (For interpretation of the references to color in this figure legend, the reader is referred to the web version of this article.)

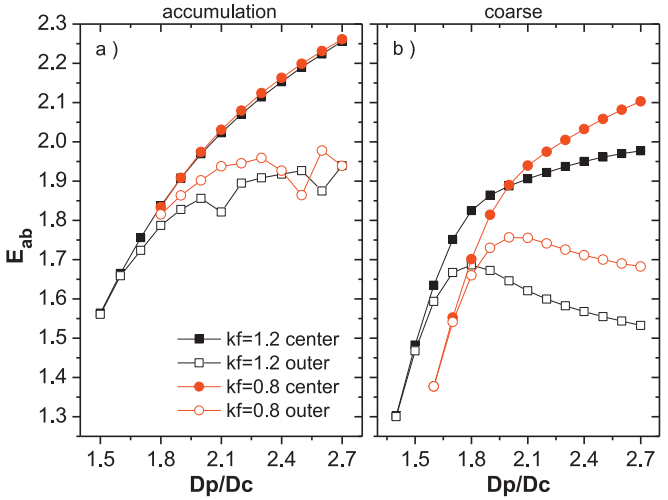

Fig. 4. Absorption enhancement (E_{ab}) of aged BC aggregates (BC fractal dimension of 2.98) for different fractal prefactors (k_f) as a function of shell/core ratio (D_p/D_c), for accumulation (left panel) and coarse (right panel) modes, respectively. Four BC coating morphologies are considered, i.e., two core-shell structures with BC mass centers located at particle geometric center having BC fractal prefactors of 1.2 (black solid squares) and 0.8 (red solid circles), and two structures with BC aggregates at an outer position close to coating boundary exhibiting BC fractal prefactors of 1.2 (black open squares) and 0.8 (red open circles). (For interpretation of the references to color in this figure legend, the reader is referred to the web version of this article.)

ture may be certainly true for some ambient aerosols. Fig. 3 shows the absorption enhancements of coated BC aggregates (BC fractal dimension of 2.8) with aforementioned size distributions for two different off-center structures in comparison with the concentric core-shell structure. For both off-center core-shell structures considered, one is BC aggregates locating at the middle of a radius of coating sphere, and the other is BC at an outer position as close as possible to the coating boundary. It is evident that the absorption enhancements of aged BC aggregates are very sensitive to the BC position inside sulfate coating. The values of E_{ab} are found to decrease as BC aggregates move from the coating center to the boundary, in consistent with the absorption results of BC-water mixture presented by Mishchenko et al. [72]. This indicates that the position of inside BC aggregates closer to coating center (overall particle geometric center) enhances BC lensing effect. Meanwhile, with BC not close to the coating boundary, less BC contents or more coating volumes also enhance BC lensing effect, since E_{ab} increases with D_p/D_c increasing. If BC aggregates are situated near the boundary of sulfate coating, E_{ab} values are within 1.8–2.0 for accumulation internal mixtures, whereas its values are generally in the range of 1.4–1.7 in coarse mode. It can be seen that BC aggregates near the boundary of heavy coating may not significantly enhance lensing effect with increased coating fraction. When sulfate coating increases from very thin layer to heavy thickness with a D_p/D_c of 2.7, the off-center core-shell structure results in E_{ab} decrease up to approximately 15% and 20% for accumulation and coarse internal mixtures, respectively, compared to the concentric aggregate core-shell structure (see Fig. 3).

Compared with the concentric spherical core-shell structure, the accumulation off-center aged BC aggregates with a BC fractal dimension of 2.8 show similar E_{ab} with differences less than 9% (combine Fig. 2 with Fig. 3). Nevertheless, in coarse mode, the off-center coated BC aggregates lead to up to 31% reductions in E_{ab} depending on BC position inside sulfate coating, and this implies that assuming a concentric spherical core-shell structure could overestimate BC absorption enhancement, and then BC radiative forcing. Adachi et al. [73] estimates that using a more realistic BC coating morphology from in-situ measurements results in around 20% less BC direct radiative forcing than using a concentric spherical core-shell structure.

The numerical investigations discussed above consider aged BC aerosols with a fixed BC fractal prefactor, while k_f can also affect the geometry of BC aggregates, in addition to D_f. Fig. 4 illustrates the absorption enhancements of coated BC aggregates (BC fractal dimension of 2.98) with aforementioned size distributions for two different BC fractal prefactors. The results with k_f of 0.8 and 1.2 for two coating structures (a concentric core-shell structure and an off-center structure with BC close to coating boundary) are compared. The effects of BC fractal prefactor on the absorption enhancements of aged BC aggregates are complicated, which are generally similar to the effects of the BC fractal dimension. This is owing to that both fractal prefactor and fractal dimension control the aggregate structure, and larger D_f or k_f increases monomer packing, which can also be seen in Eq. (1). The preceding analysis demonstrates coating morphologies exerting a significant impact on aged BC absorption enhancement. Therefore, to generate reliable estimates of BC radiative forcing from aerosol-climate models, the parameterization of realistic BC coating morphology seems to be a must, which, however, could be a challenging task due to more observations still needing to be carried out.

3.2. Effect of BC refractive index on E_{ab}

Bond et al. [55] show significant uncertainties in BC refractive indices (RIs) with an upper-bound BC RI of $1.95-0.79i$ and a lower-bound of $1.75-0.63i$. The influence of BC RI uncertainties on absorption enhancement of concentric coated BC aggregates (BC fractal dimension of 2.8) with aforementioned size distributions is illustrated in Fig. 5. The results with BC RIs at the upper and lower bounds are compared to those utilizing aforementioned BC RI of $1.85-0.71i$. Theoretical calculations show that using a BC RI of $1.95-0.79i$ increases E_{ab} of accumulation aged BC mixtures by 3–4% while using a $1.75-0.63i$ decreases E_{ab} by 3–4% for different D_p/D_c values (see Fig. 5a). The calculated E_{ab} values of coarse coated BC based on three different BC RI are in general agreement

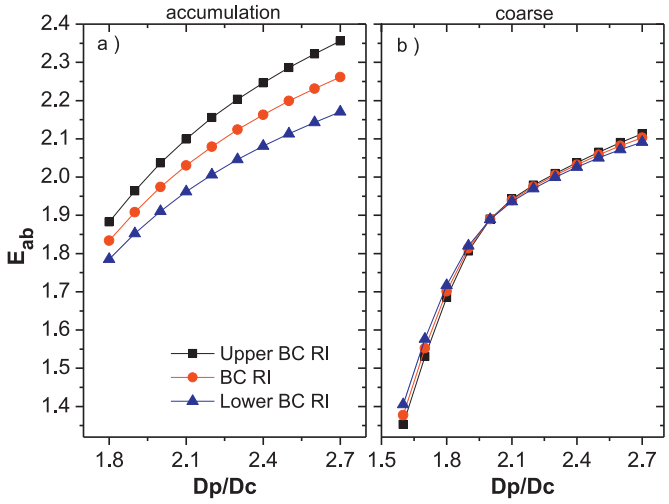

Fig. 5. Absorption enhancement (E_{ab}) of aged BC aggregates (BC fractal dimension of 2.8) with different BC refractive index as a function of shell/core ratio (D_p/D_c), for accumulation (left panel) and coarse (right panel) modes, respectively. Three BC refractive index (RIs) are considered, including a popular RI of $1.85-0.71i$ (red circles), an upper-bound RI of $1.95-0.79i$ (black squares) and a lower-bound RI of $1.75-0.63i$ (blue triangles). (For interpretation of the references to color in this figure legend, the reader is referred to the web version of this article.)

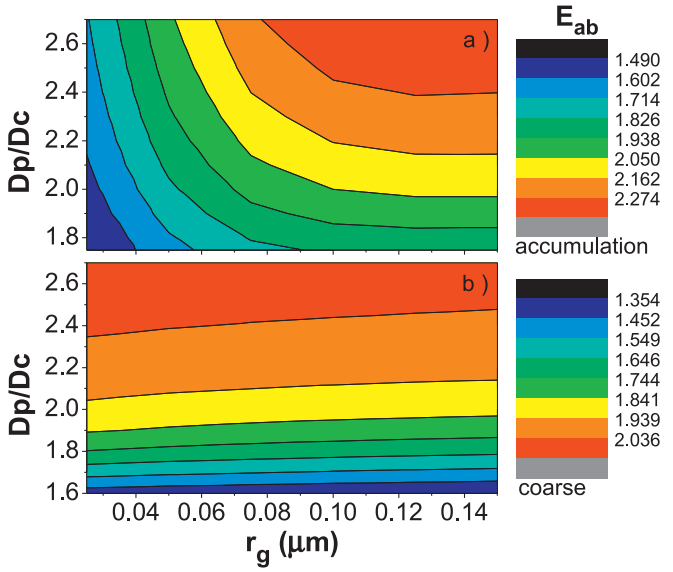

Fig. 6. Absorption enhancement (E_{ab}) of aged BC aggregates (BC fractal dimension of 2.8) with different shell/core ratio (D_p/D_c) and particle size distribution for accumulation (top panel) and coarse (bottom panel) modes, respectively. The geometric standard deviations (σ_g) for applied lognormal distribution are 1.59 and 2.0 for accumulation and coarse aerosols, respectively.

with differences less than 2% (see Fig. 5b). Using BC RIs at the upper and lower bounds, He et al. [34] find variations of 20–40% and 10–17% in absorption for fresh and coated BC aggregates, respectively. Liu at al. [51] and Scarnato et al. [74] also show that the absorption of uncoated BC aggregates have strong dependences on BC refractive index. Although BC refractive index uncertainties affect BC absorption significantly, they have little impact on absorption enhancement of coated BC aggregates with differences within 4% and 2% for accumulation and coarse modes, respectively, based on this study.

3.3. Effect of particle size distribution on E_{ab}

Fig. 6 illustrates the variations of E_{ab} for concentric coated BC aggregates (BC fractal dimension of 2.8) at different composition ratios with different size distributions. The lognormal size distributions are assumed for aged BC particles with r_g (x axis) ranging from 0.025 μm to 0.15 μm and σ_g as aforementioned values. Fig. 6 clearly depicts that E_{ab} is quite sensitive to both particle size distribution and composition ratio. As sulfate coating increases from very thin layer to heavy thickness (i.e., D_p/D_c increases), E_{ab} increases dramatically, indicating enhanced coating fraction enlarges absorption enhancement of aged BC aerosols. The E_{ab} values of accumulation aged BC aggregates decrease as r_g increases (i.e., particles becoming larger), whereas the reverse is true for coarse coated BC. Compared with the results of coarse particles, E_{ab} values of accumulation coated BC aggregates are more sensitive to particle size distribution, i.e., showing larger variation. For BC aggregates with $D_f=2.8$ fully coated with very thin sulfate, values of E_{ab} are in ranges of 1.5–1.8 and 1.3–1.4 in accumulation and coarse modes, respectively. Nevertheless, as BC particles undergo a heavy sulfate coating with $D_p/D_c=2.7$, their E_{ab} values range from 1.7–2.4 and 2.0–2.1 for accumulation and coarse mixtures, respectively. Overall, besides composition ratio, Fig. 6 indicates that the absorption enhancement of aged BC is sensitive to its size distribution, and the sensitivity of absorption enhancement to size distribution becomes stronger in accumulation mode compared to coarse mode.

The previous theoretical analysis depicts the absorption enhancement of aged BC sensitive to its microphysics (composition ratio, coating morphology, BC refractive index, and size distribution), which may have atmospheric implications. The BC aging under different atmospheric conditions may cause large variability in the coating microphysics [41,42,75,76], and thus, better characterizing the microphysics of aged BC aerosols over the world are critical to estimate their absorption enhancement and assess their radiative effect accurately. Peng et al. [77] present that BC aging exhibits two distinct stages, i.e., initial transformation from a fractal to spherical morphology and subsequent growth of fully compact particles with a large absorption enhancement, and our employed aged BC model conforms to this experimental work. Our theoretical predictions for accumulation coated BC are generally consistent with another experimental work [78], reporting significant absorption enhancement of BC aggregates after exposure to sulfuric acid at 320 nm particle size. Recent observations in a rural site in the NCP show mean E_{ab} of 2.25 [28], which may be generally captured using a fully coated BC aggregate model in our study. The high BC absorption enhancement measured in the NCP may be indicative of dominated heavily coated BC aerosols with cores not close to the coating boundary based on above analysis. As E_{ab} is source and regionally dependent [79], we suggest that a simple spherical model with BC aggregates fully coated with weakly absorbing materials may be used to describe the aged BC aerosols over the NCP in regional aerosol-climate models. However, it needs to be noticed that urban aerosols typically contain a mixture of various organic and inorganic species [80]. In addition to inorganic species, such as sulfate investigated in this study, aged BC aerosols can also contain a large mass fraction of secondary organics [81], and previous laboratory studies have shown distinct effects of organic coating on BC optical properties [82]. Thus, the absorption enhancements of BC aerosols coated with other species, such as organics, still need investigation, which will be the further studies.

4. Conclusions

The study develops a simple model to study the absorption properties of aged BC aggregates in accumulation and coarse modes calculated by the famous MSTM, and reveals the impact of aerosol microphysics on the absorption enhancement of fully coated BC. The concentric spherical core-shell structure with the

equivalent BC and coating volumes is also considered for comparison, as it is the simplest and most widely applied morphology for coated BC aerosols.

The numerical investigation yields absorption cross sections of aged BC particles sensitive to their inside BC geometries in coarse mode but not in accumulation mode. The absorption enhancement of concentric coated BC aggregates is very sensitive to BC geometry only in coarse mode, and it can alter up to 20% due to different BC fractal dimensions. The absorption enhancement of coated BC aggregates is also sensitive to the BC position inside sulfate coating, and the off-center structure can result in E_{ab} decrease up to approximately 15% and 20% in accumulation and coarse modes, respectively, compared to the concentric coated BC aggregates. Compared with the concentric spherical coated BC, the off-center coated BC aggregates shows similar E_{ab} with differences less than 9% in accumulation mode, whereas it lead to up to 31% reductions in E_{ab} in coarse mode, depending on BC position inside sulfate coating. Our study indicates that, with BC aggregates not close to the coating boundary, larger D_p/D_c (i.e., less BC content or more coating fraction) or BC position closer to particle geometric center enhance BC lensing effect. However, BC aggregates near the boundary of heavy coating may not further enhance lensing effect significantly with increased coating fraction.

The uncertainties of BC refractive index have little impact on the absorption enhancement of coated BC aggregates with differences within 4% and 2% for accumulation and coarse modes, respectively. The absorption enhancement of aged BC is also sensitive to particle size distribution, and the sensitivities are stronger in accumulation mode compared to coarse mode. The E_{ab} values of accumulation coated BC aggregates decrease as r_g increases (i.e., particles becoming larger), whereas the reverse is true for coarse coated BC. For thin concentric coated BC aggregates with BC $D_f = 2.8$, values of E_{ab} are in ranges of 1.5–1.8 and 1.3–1.4 in accumulation and coarse modes, respectively. Nevertheless, as BC particles undergo a heavy sulfate coating with $D_p/D_c = 2.7$, their E_{ab} values range from 1.7–2.4 and 2.0–2.1 for accumulation and coarse mixtures, respectively.

The aged BC aerosols have complex coating structure in the atmosphere, with fully coated BC exhibiting significant large E_{ab} depicted in our study. This indicates the significant contributions of fully coated BC particles to ambient BC absorption enhancement measured in field experiments, which shows changeability over different regions. Although the absorption enhancement aged BC aerosols have large variability due to their complicated coating microphysics, the efficient model developed in this study may be applied to describe aged BC aerosols over the NCP in regional aerosol-climate models.

Acknowledgments

This work is financially supported by the National Natural Science Foundation of China (NSFC) (Nos. 41505127, 21406189), the Natural Science Foundation of Jiangsu Province (No. BK20150901), and the Natural Science Foundation of the Jiangsu Higher Education Institutions of China (No. 15KJB170009). This work is also supported by the Startup Foundation for introducing Talent of NUIST (Nos. 2015r002, 2014r011), the China Postdoctoral Science Foundation Funded Project (No. 2016M591883), the Jiangsu Planned Projects for Postdoctoral Research Funds (No. 1601262C), the Jiangsu Government Scholarship for Overseas Studies, the NUIST Scholarship for Overseas Studies, and the Students Innovation and Entrepreneurship Training Program (201510300022Z). We particularly acknowledge the source of the codes of MSTM 3.0 from Daniel W. Mackowski. We also gratefully appreciate the supports from Special Program for Applied Research on Super Computation of the NSFC-Guangdong Joint Fund (the second phase).

References

[1] Mao M, Zhang X, Fang X, Wu G, Dai S, Song Q, et al. Highly efficient light-harvesting boradiazaindacene sensitizers for dye-sensitized solar cells featuring phenothiazine donor antenna. J Power Sources 2014;268:965–76.
[2] Mao M, Li Q, Zhang X, Wu G, Dai C, Ding Y, et al. Effects of donors of bodipy dyes on the performance of dye-sensitized solar cells. Dyes Pigments 2017;141:148–60.
[3] Intergovernmental Panel on Climate Change (IPCC). Climate Change, 2013. The physical science basis. UK: Cambridge University Press; 2013.
[4] Jacobson MZ. Effects of biomass burning on climate, accounting for heat and moisture fluxes, black and brown carbon, and cloud absorption effects. J Geophys Res 2014;119:8980–9002.
[5] Jacobson MZ. Strong radiative heating due to the mixing state of black carbon in atmospheric aerosols. Nature 2001;409(6821):695–7.
[6] Ramanathan V, Carmichael G. Global and regional climate changes due to black carbon. Nat Geosci 2008;1(4):221–7.
[7] Schnaiter M. Absorption amplification of black carbon internally mixed with secondary organic aerosol. J Geophys Res 2005;110 (D19):D19204.
[8] Shiraiwa M, Kondo Y, Iwamoto T, Kita K. Amplification of light absorption of black carbon by organic coating. Aerosol Sci Technol 2010;44(1):46–54.
[9] Liu L, Mishchenko MI. Effects of aggregation on scattering and radiative properties of soot aerosols. J Geophys Res 2005;110:D11211.
[10] Chakrabarty RK, Beres ND, Moosmuller H, China S, Mazzoleni C, Dubey MK, et al. Soot superaggregates from flaming wildfires and their direct radiative forcing. Sci Rep 2014;4:5508.
[11] Zhang RY, Khalizov AF, Pagels J, Zhang D, Xue HX, McMurry PH. Variability in morphology, hygroscopicity, and optical properties of soot aerosols during atmospheric processing. Proc Natl Acad Sci USA 2008;105:10291–6.
[12] Pagels J, Khalizov AF, McMurry PH, Zhang RY. Processing of soot by controlled sulphuric Acid and water condensation mass and mobility relationship. Aerosol Sci Tech 2009;43:629–40.
[13] Zhang RY, Khalizov A, Wang L, Hu M, Xu W. Nucleation and growth of nanoparticles in the atmosphere. Chem Rev 2012;112:1957–2011.
[14] Shiraiwa M, Kondo Y, Moteki N, Takegawa N, Miyazaki Y, Blake DR. Evolution of mixing state of black carbon in polluted air from Tokyo. Geophys Res Lett 2007;34:L16803.
[15] Kondo Y, Matsui H, Moteki N, Sahu L, Takegawa N, Kajino M, et al. Emissions of black carbon, organic, and inorganic aerosols from biomass burning in North America and Asia. J Geophys Res 2008;116:D08204 2011.
[16] Bond TC, Habib G, Bergstrom RW. Limitations in the enhancement of visible light absorption due to mixing state. J Geophys Res 2006;111:D20211.
[17] Schwarz JP, Spackman JR, Fahey DW, Gao RS, Lohmann U, Stier P, et al. Coatings and their enhancement of black carbon light absorption in the tropical atmosphere. J Geophys Res 2008;113:D03203.
[18] Cross ES, Onasch TB, Ahern A, Wrobel W, Slowik JG, Olfert J, et al. Soot particle studies—instrument inter-comparison—project overview. Aerosol Sci Technol 2010;44:592–611.
[19] Schnaiter M, Linke C, Möhler O, Naumann K-H, Saathoff H, Wagner R, et al. Absorption amplification of black carbon internally mixed with secondary organic aerosol. J Geophys Res 2005;110:D19204.
[20] Shiraiwa M, Kondo Y, Iwamoto T, Kita K. Amplification of light absorption of black carbon by organic coating. Aerosol Sci Technol 2010;44:46–54.
[21] Zhang R, Khalizov AF, Pagels J, Zhang D, Xue H, McMurry PH. Variability in morphology, hygroscopicity, and optical properties of soot aerosols during atmospheric processing. Proc Natl Acad Sci USA 2008;105:10291–6.
[22] Schwarz JP, Gao RS, Spackman JR, Watts LA, Thomson DS, Fahey DW. Measurement of the mixing state, mass, and optical size of individual black carbon particles in urban and biomass burning emissions. Geophys Res Lett 2008;35:337–44.
[23] Zhang X, Rao R, Huang Y, Mao M, Berg MJ, Sun W. Black carbon aerosols in urban central China. J Quant Spectrosc Radiat Transf 2015;150:3–11.
[24] Smith AJA, Grainger RG. Simplifying the calculation of light scattering properties for black carbon fractal aggregates. Atmos Chem Phys 2014;14:7825–36.
[25] Smith AJA, Peters DM, McPheat R, Lukanihins S, Grainger RG. Measuring black carbon spectral extinction in the visible and infrared. J Geophys Res 2015;120:9670–83.
[26] Knox A, Evans GJ, Brook JR, Yao X, Jeong CH, Godri KJ, et al. Mass absorption cross-section of ambient black carbon aerosol in relation to chemical age. Aerosol Sci Tech 2009;43:522–32.
[27] Naoe H, Hasegawa S, Heintzenberg J, Okada K, Uchiyama A, Zaizen Y, et al. State of mixture of atmospheric submicrometer black carbon particles and its effect on particulate light absorption. Atmos Environ 2009;43:1296–301.
[28] Cui X, Wang X, Yang L, Chen B, Chen J, Andersson A, et al. Radiative absorption enhancement from coatings on black carbon aerosols. Sci Total Environ 2016;551–552:51–6.
[29] Cappa CD, Onasch TB, Massoli P, Worsnop DR, Bates TS, Cross ES, et al. Radiative absorption enhancements due to the mixing state of atmospheric black carbon. Science 2012;337:1078–81.
[30] Chung SH, Seinfeld JH. Climate response of direct radiative forcing of anthropogenic black carbon. J Geophys Res 2005;110:D11102.
[31] Flanner MG, Zender CS, Randerson JT, Rasch PJ. Present-day climate forcing and response from black carbon in snow. J Geophys Res 2007;112:D11202.
[32] Wang Q, Jacob DJ, Spackman JR, Perring AE, Schwarz JP, Moteki N, et al. Global budget and radiative forcing of black carbon aerosol: constraints

from pole-to-pole (HIPPO) observations across the Pacific. J Geophys Res 2014;119:195–206.
[33] Fierce L, Bond TC, Bauer SE, Mena F, Riemer N. Black carbon absorption at the global scale is affected by particle-scale diversity in composition. Nat Commun 2016;7:12361.
[34] He C, Liou K-N, Takano Y, Zhang R, Zamora ML, Yang P, et al. Variation of the radiative properties during black carbon aging: theoretical and experimental intercomparison. Atmos Chem Phys 2015;15:11967–80.
[35] Dong J, Zhao JM, Liu LH. Morphological effects on the radiative properties of soot aerosols in different internally mixing states with sulfate. J Quant Spectrosc Radiat Transf 2015;165:43–55.
[36] Liu F, Yon J, Bescond A. On the radiative properties of soot aggregates - Part2: effects of coating. J Quant Spectrosc Radiat Transf 2015;172:134–45.
[37] Liu D, Taylor JW, Young DE, Flynn MJ, Coe H, Allan JD. The effect of complex black carbon microphysics on the determination of the optical properties of brown carbon. Geophys Res Lett 2015;42:613–19.
[38] Zhang Y, Zhang Q, Cheng Y, Su H, Kecorius S, Wang Z, et al. Measuring the morphology and density of internally mixed black carbon with SP2 and VTDMA: new insight into the absorption enhancement of black carbon in the atmosphere. Atmos Meas Tech 2016;9:1833–43.
[39] Wang G, Zhang R, Gomez ME, Yang L, Zamora ML, Hu M, et al. Persistent sulfate formation from London fog to Chinese haze. Proc Natl Acad Sci USA 2016;113(48):13630–5.
[40] Wang Q, Huang R, Cao J, Han Y, Wang G, Li G, et al. Mixing state of black carbon aerosol in a heavily polluted urban area of China: implications for light absorption enhancement. Aerosol Sci Technol 2014;48:689–97.
[41] China S, Mazzoleni C, Gorkowski K, Aiken AC, Dubey MK. Morphology and mixing state of individual freshly emitted wildfire carbonaceous particles. Nat Commun 2013;4:2122.
[42] China S, Scarnato B, Owen RC, Zhang B, Ampadu MT, Kumar S, et al. Morphology and mixing state of aged soot particles at a remote marine free troposphere site: Implications for optical properties. Geophys Res Lett 2015;42:1243–50.
[43] Adachi K, Buseck PR. Changes of ns-soot mixing states and shapes in an urban area during CalNex. J Geophys Res 2013;118:3723–30.
[44] Scarnato BV, Vahidinia S, Richard DT, Kirchstetter TW. Effects of internal mixing and aggregate morphology on optical properties of black carbon using a discrete dipole approximation model. Atmos Chem Phys 2013;13:5089–101.
[45] Liu L, Mishchenko MI. Scattering and radiative properties of complex soot and soot-containing aggregate particles. J Quant Spectrosc Radiat Transf 2007;106:262–73.
[46] Li W, Sun J, Xu L, Shi Z, Riemer N, Sun Y, et al. A conceptual framework for mixing structures in individual aerosol particles. J Geophys Res 2016;121:13784–98.
[47] Sorensen CM. Light scattering by fractal aggregates: a review. Aerosol Sci Technol 2001;35(2):648–87.
[48] Tritscher T, Juranyi Z, Martin M, Chirico R, Gysel M, Heringa MF, et al. Changes of hygroscopicity and morphology during ageing of diesel soot. Environ Res Lett 2011;6:034026.
[49] Schwarz JP, Gao RS, Spackman JR, Watts LA, Thomson DS, Fahey DW, et al. Measurement of the mixing state, mass, and optical size of individual black carbon particles in urban and biomass burning emissions. Geophys Res Lett 2008;35(13):L13810.
[50] Coz E, Leck C. Morphology and state of mixture of atmospheric soot aggregates during the winter season over Southern Asia–a quantitative approach. Tellus B 2011;63:107–16.
[51] Liu L, Mishchenko MI, Arnott WP. A study of radiative properties of fractal soot aggregates using the superposition T-matrix method. J Quant Spectrosc Radiat Transf 2008;109(15):2656–63.
[52] Alexander DTL, Crozier PA, Anderson JR. Brown carbon spheres in East Asian outflow and their optical properties. Science 2008;321:833–6.
[53] Wu Y, Cheng TH, Zheng LJ, Chen H. Optical properties of the semi-external mixture composed of sulfate particle and different quantities of soot aggregates. J Quant Spectrosc Radiat Transf 2016;179:139–48.
[54] Moffet RC, Prather KA. In-situ measurements of the mixing state and optical properties of soot with implications for radiative forcing estimates. Proc Natl Acad Sci USA 2009;106:11872–7.
[55] Bond TC, Bergstrom RW. Light absorption by carbonaceous particles: an investigative review. Aerosol Sci Technol 2006;40:27–67.
[56] Adachi K, Buseck PR. Internally mixed soot, sulfates, and organic matter in aerosol particles from Mexico City. Atmos Chem Phys 2008;8:6469–81.
[57] Skorupski K, Mroczka J, Wriedt T, Riefler N. A fast and accurate implementation of tunable algorithms used for generation of fractal-like aggregate models. Physica A 2014;404:106–17.
[58] Mackowski DW. A general superposition solution for electromagnetic scattering by multiple spherical domains of optically active media. J Quant Spectrosc Radiat Transf 2014;133:264–70.
[59] Mackowski DW, Mishchenko MI. Calculation of the T matrix and the scattering matrix for ensembles of spheres. J Opt Soc Am A 1996;13:2266–78.
[60] Dlugach JM, Mishchenko MI. Scattering properties of heterogeneous mineral aerosols with absorbing inclussions. J Quant Spectrosc Radiat Transf 2015;162:89–94.
[61] Mishchenko MI, Dlugach JM, Yurkin MA, Bi L, Cairns B, Liu L, et al. First-principles modeling of electromagnetic scattering by discrete and discretely heterogeneous random media. Phys Rep 2016;632:1–75.
[62] Yurkin MA, Hoekstra AG. The discrete dipole approximation: an overview and recent developments. J Quant Spectrosc Radiat Transf 2007;106:558–89.
[63] Zhang K, O'Donnell D, Kazil J, Stier P, Kinne S, Lohmann U, et al. The global aerosol-climate model ECHAM-HAM, version 2: sensitivity to improvements in process representations. Atmos Chem Phys 2012;12:8911–49.
[64] Yu F, Luo G. Simulation of particle size distribution with a global aerosol model: contribution of nucleation to aerosol and CCN number concentrations. Atmos Chem Phys 2009;9:7691–710.
[65] Zhang X, Huang Y, Rao R. Aerosol characteristics including fumigation effect under weak precipitation over the southeastern coast of China. J Atmos Sol-Terr Phy 2012;84–85:25–36.
[66] Zhang X, Huang Y, Rao R, Wang Z. Retrieval of effective complex refractive index from intensive measurements of characteristics of ambient aerosols in the boundary layer. Opt Express 2013;21(15):17849–62.
[67] Zhang X, Huang Y, Zhu W, Rao R. Aerosol characteristics during summer haze episodes from different source regions over the coast city of North China Plain. J Quant Spectrosc Radiat Transf 2013;122:180–93.
[68] Zhang X, Mao M, Berg MJ, Sun W. Insight into wintertime aerosol characteristics over Beijing. J Atmos Sol-Terr Phy 2014;121:63–71.
[69] Zhang X, Mao M. Brown haze types due to aerosol pollution at Hefei in the summer and fall. Chemosphere 2015;119:1153–62.
[70] Aouizerats B, Thouron O, Tulet P, Mallet M, Gomes L, Henzing JS. Development of an online radiative module for the computation of aerosol optical properties in 3-D atmospheric models: validation during the EUCAARI campaign. Geosci Model Dev 2010;3:553–64.
[71] Kahnert M, Nousiainen T, Lindqvist H. Models for integrated and differential scattering optical properties of encapsulated light absorbing carbon aggregates. Opt Express 2013;21:7974–93.
[72] Mishchenko MI, Liu L, Cairns B, Mackowski DW. Optics of water cloud droplets mixed with black-carbon aerosols. Opt Lett 2014;39:2607–10.
[73] Adachi K, Chung SH, Buseck PR. Shapes of soot aerosol particles and implications for their effects on climate. J Geophys Res 2010;115:D15206.
[74] Scarnato BV, China S, Nielsen K, Mazzoleni C. Perturbations of the optical properties of mineral dust particles by mixing with black carbon: a numerical simulation study. Atmos Chem Phys 2015;15:6913–28.
[75] Moteki N, Kondo Y, Miyazaki Y, Takegawa N, Komazaki Y, Kurata G, et al. Evolution of mixing state of black carbon particles: aircraft measurements over the western Pacific. March 2004. Geophys Res Lett 2007;34:L11803.
[76] Metcalf AR, Craven JS, Ensberg JJ, Brioude J, Angevine W, Sorooshian A, et al. Black carbon aerosol over the Los Angeles basin during CalNex. J Geophys Res 2012;117 D00v13.
[77] Peng J, Hua M, Guo S, Du Z, Zheng J, Shang D, et al. Markedly enhanced absorption and direct radiative forcing of black carbon under polluted urban environments. Proc Natl Acad Sci USA 2016;113:4266–71.
[78] Khalizov AF, Xue H, Wang L, Zheng J, Zhang R. Enhanced light absorption and scattering by carbon soot aerosols internally mixed with sulfuric acid. J Phys Chem 2009;113:1066–74.
[79] Liu S, Aiken AC, Gorkowski K, Dubey MK, Cappa CD, Williams LR, et al. Enhanced light absorption by mixed source black and brown carbon particles in UK winter. Nat Commun 2015;6:8435.
[80] Guo S, Hua M, Zamora ML, Peng J, Shang D, Zheng J, et al. Elucidating severe urban haze formation in China. Proc Natl Acad Sci USA 2014;111:17373–8.
[81] Zhang R, Wang G, Guo S, Zamora ML, Ying Q, Lin Y, et al. Formation of urban fine particulate matter. Chem Rev 2015;115:3803–55.
[82] Xue H, Khalizov AF, Wang L, Zheng ZR. Effects of dicarboxylic acid coating on the optical properties of soot. Phys Chem Chem Phys 2009;11:7865–75.